

Description of the superdeformed band of ^{36}Ar with the Gogny force

R.R. Rodríguez-Guzmán

*Institut für Theoretische Physik der Universität Tübingen,
Auf der Morgenstelle 14, D-72076 Tübingen, Germany.*

J.L. Egido and L.M. Robledo

*Departamento de Física Teórica C-XI, Universidad Autónoma de Madrid
Madrid 28049, Spain
J.Luis.Egido@uam.es, Luis.Robledo@uam.es*

Received (received date)

Revised (revised date)

The superdeformed band of ^{36}Ar is studied with the Gogny force D1S and the angular momentum projected generator coordinate method for the quadrupole moment. The band head excitation energy, moments of inertia, $B(E2)$ transition probabilities and stability against quadrupole fluctuations at low spin are studied. The Self Consistent Cranking method is also used to describe the superdeformed rotational band. In addition, properties of some normal deformed states are discussed.

1. Introduction.

The lightest atomic nucleus known up to now to have a superdeformed band (SD) is ^{36}Ar ¹. The use of the sophisticated GAMMASPHERE array detector has allowed the determination of the excitation energy of the members of its SD band¹ up to $I = 16\hbar$ (which is thought to be the highest possible value of the band) as well as the in-band and some out-band $B(E2)$ transition probabilities². Theoretical analyses indicate that the appearance of the SD band is linked to the excitation of four particles from the sd shell into the fp one^{1,2,3}. In addition, a normal deformed oblate band is also known⁴. In the theoretical side, this SD band has been studied with the Cranked Nilsson-Strutinsky (CNS) and shell model approaches^{1,2}, the Projected Shell Model (PSM)⁵ and with angular momentum projected techniques with the Skyrme SLy6 interaction⁶.

The purpose of this paper is to study, using the Gogny interaction⁷ with the D1S parameterization⁸, the properties of the SD of the nucleus ^{36}Ar focusing on the stability of the SD minimum against quadrupole fluctuations at low spin. The reason is that in some of the theoretical studies mentioned in the above paragraph the SD minimum observed in the energy landscape was very shallow rising serious doubts about its ability to hold states at low angular momentum when fluctuations

in the quadrupole degree of freedom are taken into consideration (see ⁹ for a discussion of this issue). Obviously, at higher spins the rotational energy makes the SD minimum deeper and therefore much more stable against quadrupole fluctuations. As a side product of our calculations we have studied the properties of low lying normal deformed states and compared them with the available experimental data. To perform the theoretical analysis, we have used the Angular Momentum Projected Generator Coordinate Method (AMP-GCM) with the axial quadrupole moment as generating coordinate and restricted ourselves to $K = 0$ configurations (see ¹⁰ for a thorough discussion of the method and ¹¹ for an application to the study of SD bands). The properties of the superdeformed band obtained with the AMP-GCM are also compared with those of a Self Consistent Cranking calculation.

2. Theoretical framework.

As we have already seen in many examples^{10,11}, whenever the quadrupole degree of freedom plays a role in the nuclear dynamics it is convenient to restore the broken rotational symmetry by projecting onto good angular momentum. The effect of angular momentum projection in the energy landscape can substantially change the mean field outcome and it turns out that in many cases several minima appear with comparable energies. As a consequence, configuration mixing of the quadrupole degree of freedom could be important. In this paper we have taken into account both angular momentum projection and configuration mixing in the framework of the Angular Momentum Projected Generator Coordinate Method (AMP-GCM). In this approach the wave functions of the system are postulated to be

$$|\Phi_\sigma^I\rangle = \int dq_{20} f_\sigma^I(q_{20}) \hat{P}_{00}^I |\varphi(q_{20})\rangle. \quad (1)$$

In this expression $|\varphi(q_{20})\rangle$ is the set of axially symmetric (i.e. $K = 0$) Hartree-Fock-Bogoliubov (HFB) wave functions generated with the constraint $\langle\varphi(q_{20})|z^2 - 1/2(x^2 + y^2)|\varphi(q_{20})\rangle = q_{20}$ on the mass quadrupole moment. The HFB wave functions are expanded in an axially symmetric Harmonic Oscillator (HO) basis with 10 major shells (220 HO states) and equal oscillator lengths in order to preserve the rotational invariance of the basis. In the evaluation of the HFB wave functions the Gogny force is used (D1S parameterization). Other details concerning the HFB calculation are the following: a) The two body kinetic energy correction is fully taken into account in the variational process. b) The Coulomb exchange part of the interaction, evaluated in the Slater approximation, has been considered in the variational process c) Reflection symmetry is imposed as a selfconsistent symmetry of our HFB wave functions.

The angular momentum projector operator

$$\hat{P}_{00}^I = \frac{2I+1}{8\pi^2} \int d\Omega d_{00}^I(\beta) e^{-i\alpha J_z} e^{-i\beta J_y} e^{-i\gamma J_z} \quad (2)$$

is the usual one restricted to axially symmetric $K = 0$ intrinsic configurations ^{12,13} and $f_\sigma^I(q_{20})$ are the “collective amplitudes” which are obtained as the solutions of

the Hill-Wheeler (HW) equation

$$\int dq'_{20} \mathcal{H}^I(q_{20}, q'_{20}) f_\sigma^I(q'_{20}) = E_\sigma^I \int dq'_{20} \mathcal{N}^I(q_{20}, q'_{20}) f_\sigma^I(q'_{20}). \quad (3)$$

The solution of the HW equation for each value of the angular momentum I determines not only the ground state ($\sigma = 1$), which is a member of the Yrast band, but also excited states ($\sigma = 2, 3, \dots$) that, in the present context, may correspond to states with different deformation than the ground state and/or quadrupole vibrational excitations.

Further technical details pertaining the evaluation of the hamiltonian kernels for density dependent forces and the evaluation of transition probabilities in the present framework are given in ¹⁰.

3. Discussion of the results.

In Figure 1 we present the results of the HFB calculations used to generate the intrinsic states $|\varphi(q_{20})\rangle$. On the left hand side of the figure we show the HFB energy (panel (a)) along with the q_{40} deformation parameter (panel (b)) and the particle-particle pairing energy $E_{pp} = -1/2\text{Tr}(\Delta\kappa^*)$ (panel (c)) for protons and neutrons (the two curves are indistinguishable) as a function of the quadrupole moment q_{20} . The energy curve shows a deformed ground state minimum at $q_{20} = -0.45\text{b}$ ($\beta_2 = -0.18$) which is only 518 keV deeper than the spherical configuration. A very shallow super deformed (SD) minimum at $q_{20} = 1.4\text{b}$ ($\beta_2 = 0.52$) is also observed at an excitation energy $E_x^{HFB}(SD) = 8.09\text{MeV}$. The depth of the SD well is very small (only 67 keV) and makes mandatory a study of the stability of such intrinsic state against quadrupole fluctuations. To study the effect of the finite size of the basis in the HFB energies and in the excitation energy of the SD minimum we have carried out calculations including 18 major shells for the HO basis^a (1140 states) for both the normal deformed (ND) and SD HFB minima and found that the corresponding energies are shifted downwards by 906 keV and 1296 keV respectively. As a consequence, the excitation energy of the SD minimum gets reduced by 390 keV up to the value $E_x^{HFB}(SD) = 7.7\text{ MeV}$.

The hexadecapole deformation parameter q_{40} increases with increasing quadrupole moments and reach at the SD minimum the rather high value $\beta_4 = 0.24$. Concerning the particle-particle correlation energies E_{pp} we observe that their values for protons and neutrons are nearly identical and they go to zero in both the normal deformed and superdeformed minima. This implies that dynamical pairing effects could be relevant for the description of both the ND and SD bands. On the right hand side of the figure we have plotted the matter density contour plots (at a density $\rho_0 = 0.08\text{fm}^{-3}$) for several values of q_{20} . Only for q_{20} values greater or equal 2.6 b the matter density distribution resembles the one corresponding to two

^aThis basis is considered by some authors ⁹ as almost indistinguishable from an infinite basis for nuclei around A=40.

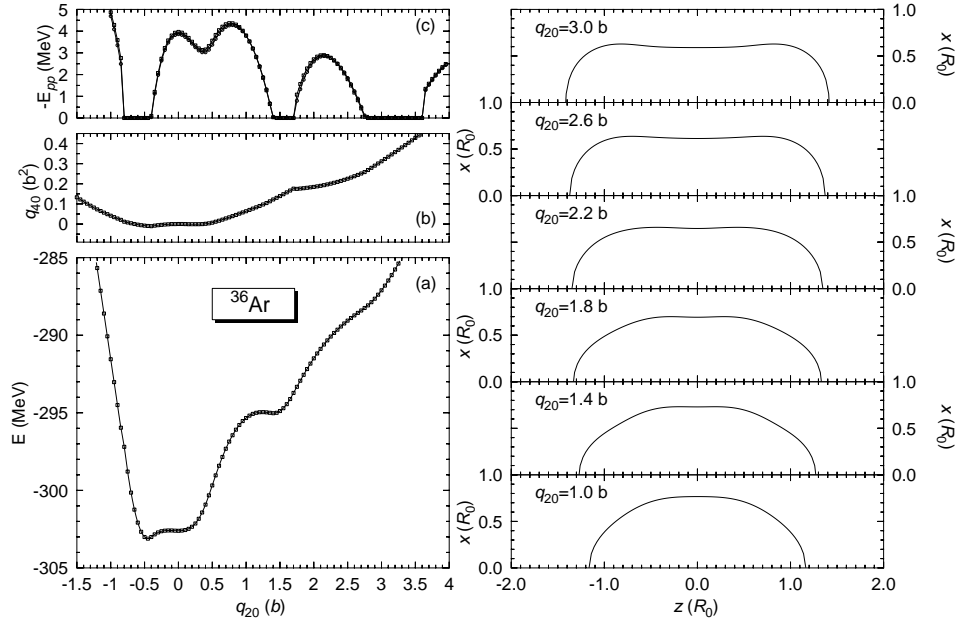


Fig. 1. On the left hand side the HFB energy in MeV (panel (a)), the q_{40} deformation parameter in b^2 (panel (b)) and the particle-particle correlation energies E_{pp} for protons and neutrons in MeV (panel (c)) are depicted as a function of the quadrupole moment q_{20} given in barns. On the right hand side, contour plots of the matter distribution corresponding to a density of 0.08 fm^{-3} and different quadrupole moments are depicted in units of $R_0 = 1.2 A^{1/3} (3.96) \text{ fm}$.

separated nuclei connected by a rather thick neck. Interestingly, this value of q_{20} corresponds to a shoulder in the HFB energy landscape that will be analyzed later on when the effect of angular momentum projection is considered.

To further study the physical contents of the ND and SD intrinsic wave functions we have computed the spherical shell occupancies $\nu(nlj) = \sum_m \langle \varphi | c_{nljm}^+ c_{nljm} | \varphi \rangle$ for each of these intrinsic wave function. These quantities give the occupancy (or contents) of the HO orbital nlj in the intrinsic wave function $|\varphi\rangle$. For the SD intrinsic state, the positive parity level occupancies are 5.26, 1.50 and 0.76 for the $1d_{5/2}$, $1d_{3/2}$ and $2s_{1/2}$ orbitals, respectively, whereas for the negative parity levels the occupancies are 1.05, 0.15, 0.83 and 0.18 for the $1f_{7/2}$, $1f_{5/2}$, $2p_{3/2}$ and $2p_{1/2}$ orbitals, respectively (the quantities for proton and neutrons are very similar and only the neutron values are given). Therefore we have for the SD intrinsic state 15.04 particles in the $N = 2$ major shell and 4.42 in the $N = 3$ one in good agreement with the shell-model results¹. It has to be mentioned, however, that the $1d_{5/2}$ is not fully occupied in our calculations in opposition to the shell model assumptions¹. On the other hand, the occupancy of the fp shell in the ND minimum is negligible as expected.

In Figure 2 we have plotted the AMP energy curves for $I = 0, \dots, 10\hbar$ (full lines)

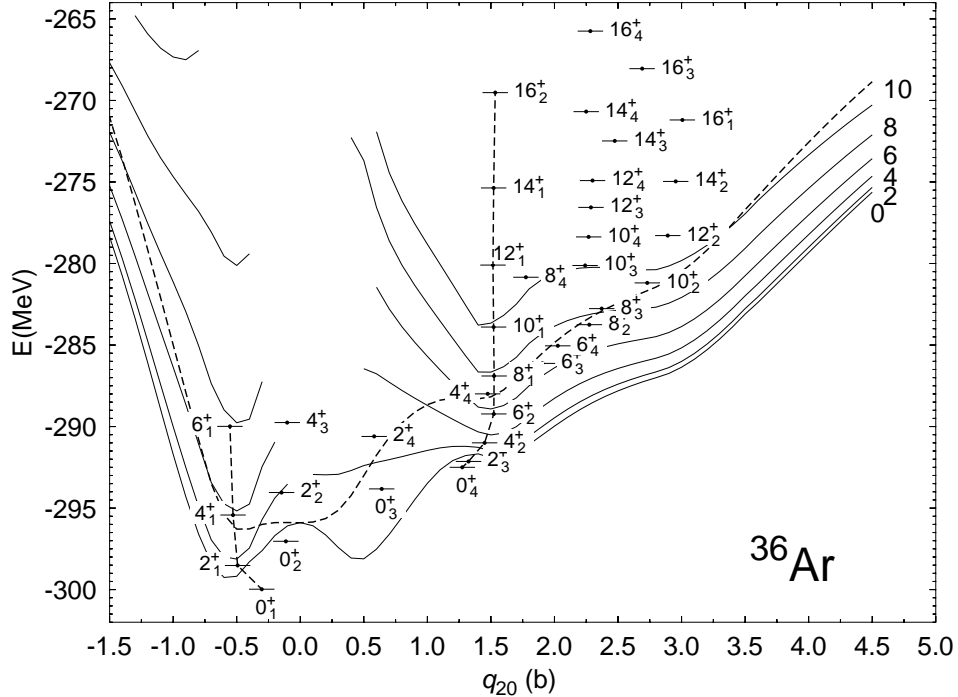


Fig. 2. The HFB energy (dashed line) and the angular momentum projected energies up to $I = 10\hbar$ are plotted as a function of the quadrupole deformation q_{20} measured in barns. The four lowest-lying solutions of the AMP-GCM equation are also plotted for each spin. The Coulomb exchange energy in the Slater approximation has not been added to the projected energy. See text for further details.

along with the HFB energy curve (dashed line) as a function of the quadrupole moment. The AMP $I = 0\hbar$ energy curve shows more pronounced ND and SD minima than the HFB one. They are located at the quadrupole moments $q_{20} = -0.55$ b and $q_{20} = 1.55$ b, respectively. The excitation energy of the SD minimum with respect to the ground state for $I = 0\hbar$ is $E_x^{AMP}(SD) = 7.37$ MeV to be compared with the 8.09 MeV obtained in the HFB calculation. Let us mention that performing the AMP calculations with 18 shells is extremely time consuming and therefore we will just use in this case the 390 keV shift obtained in the HFB to account for the effect of the finite size of the basis in the excitation energy of the SD band head. If we take into consideration the 390 keV shift the excitation energy of the SD minimum in the AMP case becomes $E_x^{AMP}(SD) = 6.98$ MeV to be compared with the 7.7 MeV obtained in the HFB case with 18 shells. We notice that for increasing spins, the superdeformed minimum gets more and more pronounced and becomes the ground state at spin $I = 8\hbar$.

We also show in Figure 2 the energies obtained in the AMP-GCM calculation for the four lowest-lying solutions of the HW equation (labeled with the subindex

Experiment			Theory		
J^π	E (MeV)	$B(E2) \downarrow (e^2 \text{fm}^4)$	J^π	E (MeV)	$B(E2) \downarrow (e^2 \text{fm}^4)$
0^+	0.00	—	0_1^+	0.00	—
2^+	1.97	60 ± 6	2_1^+	1.45	72.1
4^+	4.41		4_1^+	4.54	102.3
6^+	9.18		6_1^+	10.01	112.8

Table 1. Excitation energies and $B(E2, I \rightarrow I - 2)$ values of the normal deformed oblate band.

$\sigma = 1, \dots, 4$) and spins from zero up to $16\hbar$. Each level has been placed at a q_{20} value corresponding to its average intrinsic deformation $(\bar{q}_{20})_\sigma^I$ (see ¹⁰ for its definition). An oblate ND band (states 0_1^+ , 2_1^+ , 4_1^+ and 6_1^+ , joined by a dotted line) is clearly observed together with a SD band (0_4^+ , 2_3^+ , 4_2^+ , 6_2^+ , 8_1^+ , etc) that becomes Yrast at angular momentum $8\hbar$. Many hyperdeformed states are also observed for spins greater or equal 8 and their appearance is linked to the shoulder observed in the HFB energy landscape at $q_{20} = 2.6$ b that becomes a minimum in the AMP energy landscapes at $I = 8\hbar$.

The binding energy obtained for the AMP-GCM (adding the Coulomb exchange energy in the Slater approximation and taking into account the 906 keV shift due to the finite size of the basis) is 307.606 MeV in very good agreement with the experimental value of 306.715 MeV. This result has to be compared with the HFB value of 304.020 MeV.

The ND band results compare well with the experimental data (see Table 1) both for the excitation energies and $B(E2)$ transition probabilities.

Concerning the SD band the first noticeable fact is that, in spite of the small depth of the SD well, the quadrupole fluctuations preserve the SD intrinsic state. Obviously the mixing with other quadrupole configurations reduces the deformation of the 0_4^+ intrinsic state as compared to the one of the HFB method but not substantially. As a consequence of configuration mixing the excitation energy of the SD band becomes 7.476 MeV (7.086 MeV including the 390 keV shift due to the finite size of the basis) which is far from the experimental value of 4.33 MeV. It is not clear whether the discrepancy should be attributed to the interaction used (rather unlikely, as the same kind of disagreement is also obtained with the Skyrme SLy6 interaction ⁶ where the SD band-head is predicted at 5.9 MeV) or to other degrees of freedom not taken into account like triaxiality or even octupolarity.

Coming back to the SD band, the calculated excitation energies compare pretty well with experiment up to the back-bending observed at $I = 10\hbar$ but the $B(E2) \downarrow$ transition probabilities come up too high. The result for the $B(E2)$ can be understood by looking at the results of the CNS calculations of ref. ¹ where it is observed that already at moderate spins the SD band members become triaxial and their deformation decreases as a function of spin. In our calculations, which do not in-

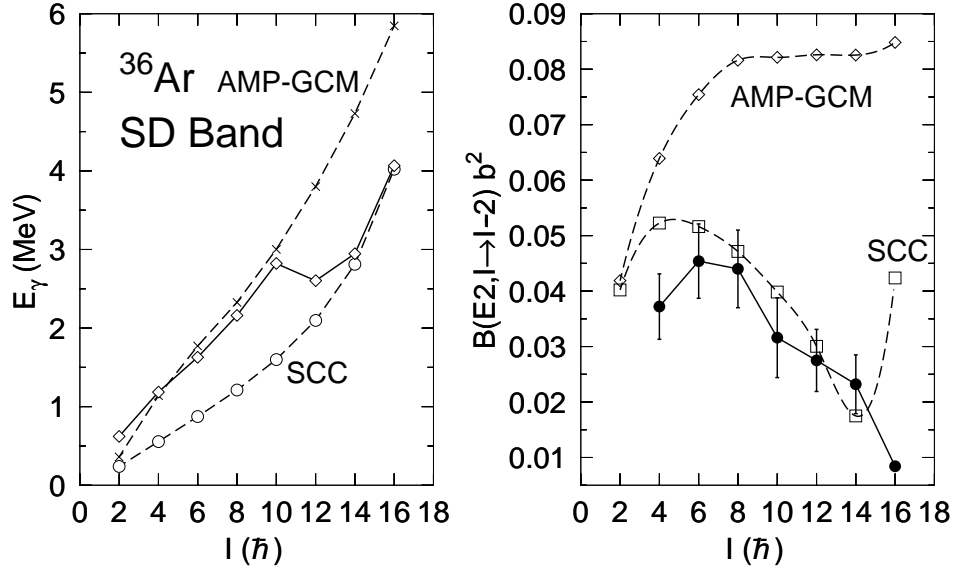


Fig. 3. In the left hand side the gamma ray energies $E_\gamma(I) = E(I) - E(I-2)$ in MeV for the SD configuration are depicted as a function of spin $I(\hbar)$ for the AMP-GCM and SCC calculations (dashed lines) along with the experimental results (full line). In the right hand side both the theoretical (AMP-GCM and SCC) and experimental results for the $B(E2, I \rightarrow I-2)$ transition probabilities in units of $e^2 b^2$ are depicted as a function of spin.

clude triaxiality, the SD band intrinsic deformation remains constant from spin $6\hbar$ on explaining the rigid rotor behavior for the $B(E2)$'s. To study the effect of triaxiality we have performed Self Consistent Cranking (SCC) calculations for the SD band and observed rather strong triaxiality effects even at zero spin and a steady decrease of deformation with increasing angular momentum (from $\beta_2 = 0.52$ at zero spin down to $\beta_2 = 0.4$ at spin $16\hbar$).

In Fig. 3 we have summarized the results of both the AMP-GCM and SCC calculations and compared them with the experimental data. We observe that the SCC results for the last two members of the SD band agree well with the experiment but for lower spins the theoretical γ ray energies are too low. This is a consequence of the lack of dynamical pairing in our calculations. Pairing correlations are zero at the SD intrinsic configuration in our calculations producing a too high moment of inertia (see ⁵ for a discussion of the pairing properties of this SD band). It is to be expected that the inclusion of dynamical pairing in our calculations will reduce the moment of inertia substantially bringing theory and experiment in much better agreement. At high spins it is expected that pairing correlations will be strongly suppressed by the Coriolis anti-pairing effect and therefore our no-pairing results agree well with the experiment in that region. Concerning the $B(E2)$ transition probabilities we observe a nice agreement between the SCC results and the experiment as well as the strong discrepancy between the AMP-GCM values and the experimental results.

From the comparison of the $B(E2)$ values it is clear that the SCC is far superior than the AMP-GCM method for the description of the SD band as it takes into account triaxial effects responsible for the decreasing of deformation with increasing spins. Therefore, we can consider that the nice agreement between the AMP-GCM excitation energies and the experiment is accidental and probably due to the fact that further improvements of the AMP-GCM will cancel out: in one hand, the dynamical pairing correlations that should decrease the moment of inertia and in the other the consideration of $\Delta K \neq 0$ admixtures in the intrinsic wave function that should increase the moment of inertia (see the discussion of this effect in ¹⁴). However, in spite of the above deficiencies, it has to be pointed out that one of the merits of the AMP-GCM is that is the only method able to asses the stability of the SD intrinsic configuration at low spins.

4. Conclusions

We have analyzed the ND and SD bands of ^{36}Ar in the framework of the Angular Momentum Projected Generator Coordinate Method (AMP-GCM) and the Self Consistent Cranking (SCC) approach. The AMP-GCM permit us to asses the stability against quadrupole deformation of the SD minimum at low spin and also allows a nice description of the ND band. For the SD band, the expected triaxiality downgrades the quality of the AMP-GCM description but we have found that the SCC is in this case rather satisfactory.

5. Acknowledgments.

This work has been supported in part by the DGI, Ministerio de Ciencia y Tecnología (Spain), under project BFM2001-0184.

References

1. C.E. Svensson et al., Phys. Rev. Lett. **85**, 2693 (2000)
2. C.E. Svensson et al., Phys. Rev. **C63**, 061301 (2001)
3. H. Röpke, J. Brenneisen and M. Lickert, Eur. Phys. J. **A14**, 159 (2002)
4. P. M. Endt, Nucl. Phys. **A521**, 1 (1990)
5. G-L Long and Y. Sun, Phys. Rev. **C63**, 021305 (2001)
6. M. Bender, H. Flocard and P.-H. Heenen, arXiv preprint: nucl-th/0305021
7. J. Dechargé and D. Gogny, Phys. Rev. **C21**, 1568 (1980)
8. J.F.Berger, M. Girod and D. Gogny, Nucl. Phys. **A428**, 23c (1984)
9. H. Molique, J. Dobaczewski and J. Dudek, Phys. Rev. **C61**, 044304 (2000)
10. R. Rodríguez-Guzmán, J.L. Egido and L.M. Robledo, Nucl. Phys. **A709**, 201(2000)
11. R. Rodríguez-Guzmán, J.L. Egido and L.M. Robledo, Phys. Rev. **C62**, 054308 (2000)
12. P. Ring and P. Schuck, *The Nuclear Many Body Problem* (Springer, Berlin, 1980).
13. K. Hara and Y. Sun, Int. J. Mod. Phys. **E4**, 637 (1995)
14. R. Rodríguez-Guzmán, J.L. Egido and L.M. Robledo, Phys. Rev. **C62**, 054319 (2000)